

Augmenting MRI scan data with real-time predictions of glioblastoma brain tumor evolution using exponential time integrators

Magdalena Pabisz¹, Judit Muñoz-Matute^{2,3}, Maciej Paszyński¹

¹ *AGH University of Krakow, Poland*

² *The Basque Center for Applied Mathematics (BCAM), Bilbao, Spain*

³ *The Oden Institute for Computational Engineering and Sciences,
The University of Texas at Austin, USA*

Abstract

We present an ultra-fast simulator to augment the MRI scan imaging of glioblastoma brain tumors with predictions of future evolution. We consider the glioblastoma tumor growth model based on the Fisher-Kolmogorov diffusion-reaction equation with logistic growth. For the discretization we employ finite differences in space coupled with a time integrator in time employing the routines from [2] to compute the actions of the exponentials of the linear operator. By combining these methods, we can perform the prediction of the tumor evolution for several months forward within a couple of seconds on a modern laptop. This method does not require HPC supercomputing centers, and it can be performed on the fly using a laptop with Windows 10, Octave simulations, and ParaView visualization. We illustrate our simulations by predicting the tumor growth evolution based on three-dimensional MRI scan data.

Keywords: Glioblastoma brain tumor, MRI scan data, Prediction of tumor evolution, Exponential time integrators

1. Introduction

Glioblastoma is a malignant brain tumor with a high mortality rate [7]. This tumor is highly aggressive, and it generates microvascular proliferation that is not visible on MRI scans [20]. Thus, computer-based simulation predictions of the evolution of the brain tumor are important in planning

treatment and surgery. But highly efficient simulators of the tumor growth take several minutes to compute a single time step [12, 24, 23, 11]. The Physics Informed Neural Networks originally proposed by Karniadakis et al. [18, 4, 3] instantiated for the brain tumor simulation in [22] can predict the future behavior of the glioblastoma tumor evolution within one hour for the patient-specific case.

In this work, we present a computational tool to perform ultra-fast simulations of three dimensional progression of glioblastoma brain tumor models. We consider the Fisher-Kolmogorov diffusion-reaction equation with logistic growth [21] describing the evolution of glioblastoma tumor in a non-homogenous environment of the human head. Our simulations employs the MRI scan data consisting of 29 bitmaps, with pixel's intensity varying from 0 to 255. We introduce materials such as skull, skin, white matter, gray matter, and air, based on the pixels intensity.

For the discretization of the transient semilinear model we combine two methods. First, we semidiscretize the space variable employing finite differences. Then, we discretize the resulting semilinear system of ordinary differential equations by an exponential integrator method [8]. For simplicity, we focus on the exponential Euler method which is first order but the extension to higher order exponential-based methods in time is straightforward. We employ the routine presented in [2] for computing the action of the corresponding ϕ -functions over vector. Then, we post-process the results and we use ParaView for visualization. We test this strategy on both 2D and 3D non-stationary glioblastoma models employing MRI data for the diffusion coefficient. The numerical results show that we can perform 100 iterations over $32 \times 32 \times 32$ computational mesh in less than 3 seconds on a laptop. Thus, this simulator can be employed "on the fly".

The efficiency comes from the fact that the exponential routines are extremely efficient on operators coming from a semidiscretization in space employing finite differences. Moreover, the exponential time integrators [9, 16, 5] are designed to solve semilinear problems that the one presented in this article. They are suitable for long-time simulations and they are unconditionally stable. From the authors understanding, there is only one work in the literature [13] where the authors employ exponential time integrators for the simulation of cancer models. This article aims to underscore the potential of this tool in the simulation of glioblastomas in the human brain.

Our future work will include development of the parallel version of the simulator, targeting GPGPU cards. This will allow us to perform simula-

tions on high resolution data of the brain. We also plan to incorporate the drug delivery into our model [15]. Having the chemotherapy included into our simulator, we plan to attack the data assimilation problem using the supermodeling technique [17, 19].

2. Glioblastoma tumor model

Let $\Omega \subset \mathbb{R}^3$ an open set and $I = (0, T)$ with $T > 0$, we consider the following Fisher-Kolmogorov diffusion-reaction equation with logistic growth [21] describing the brain tumor dynamics.

$$\left\{ \begin{array}{l} \frac{\partial \mathbf{u}}{\partial t} = \underbrace{\nabla \cdot (\mathbf{D}(\mathbf{x}) \nabla \mathbf{u})}_{\text{Tumor cell diffusion}} + \underbrace{\rho \mathbf{u}(1 - \mathbf{u})}_{\text{Tumor cell proliferation}}, \quad \text{in } \Omega \times I, \\ \nabla \mathbf{u} \cdot \mathbf{n} = 0, \quad \text{on } \partial\Omega \times I, \\ \mathbf{u}(\mathbf{x}, 0) = \mathbf{u}_0, \quad \text{on } \Omega \times \{0\}. \end{array} \right. \quad (1)$$

Here, $\mathbf{u}(\mathbf{x}, \mathbf{y}, \mathbf{z}; \mathbf{t})$ represents the tumor cell density scalar field, and $\mathbf{D}(\mathbf{x}, \mathbf{y}, \mathbf{z})$ represents the diffusion coefficient, describing how the tumor cells expand in a tissue, similarly to the diffusion phenomena. The ρ coefficient describes the proliferation rate of the tumor cells (how fast they multiply). Modeling the tumor cell dynamics by this kind of PDE results in a progression of the tumor "traveling wave" with the velocity $2\sqrt{\mathbf{D}\rho}$, according to [22].

The diffusion coefficient usually patient-specific. Following [6], it expressed as a linear combination of gray and white matter coefficients, namely $\mathbf{D} = \mathbf{p}_w \mathbf{D}_w + \mathbf{p}_g \mathbf{D}_g$, where $\mathbf{p}_w, \mathbf{p}_g$ corresponds to the proportions of the white and gray matter, obtained from the MRI scans. Here, we considered the case of isotropic diffusion in both the white and the grey matter [10]. Following [14] and [22], we assume that $\mathbf{D}_w = 10\mathbf{D}_g$, and we select $\mathbf{D}_w = 0.13$ [$\text{mm}^2\text{days}^{-1}$], $\mathbf{D}_g = 0.013$ [$\text{mm}^2\text{days}^{-1}$]. Moreover, following [6] we set $\rho = 0.025$ [days^{-1}]. With this setup, assuming 70 percent of the gray matter and 30 percent of the white matter, we expect the tumor growth to progress with a velocity of $2\sqrt{\mathbf{D}\rho} = 2\sqrt{\mathbf{p}_w \mathbf{D}_w + \mathbf{p}_g \mathbf{D}_g} \rho = 0.11$ [mm days^{-1}]. Thus, we expect the tumor to progress to 11 mm per 100 days.

3. Finite differences

We first semi-discretize (1) in space employing finite differences. Namely, we introduce a regular grid with equidistant points in each spatial direction:

$$\{\mathbf{x}_{i,j,k} = ((i-1)\mathbf{h}, (j-1)\mathbf{h}, (k-1)\mathbf{h})\}_{i=1,\dots,N_x; j=1,\dots,N_y; k=1,\dots,N_z}, \quad (2)$$

and we represent the values of the tumor cell densities at these point at time moment t as

$$\{\mathbf{u}_{i,j,k}^t = \mathbf{u}(\mathbf{x}_{i,j,k}; t)\}_{i=1,\dots,N_x; j=1,\dots,N_y; k=1,\dots,N_z}. \quad (3)$$

We discretize the equation at time moment t using finite differences as follows

$$\begin{aligned} \frac{\partial \mathbf{u}_{i,j,k}^t}{\partial t} &= \frac{\partial D(\mathbf{x}_{i,j,k})}{\partial x_1} \frac{\partial \mathbf{u}_{i,j,k}^t}{\partial x_1} + D(\mathbf{x}_{i,j,k}) \frac{\partial^2 \mathbf{u}_{i,j,k}^t}{\partial x_1^2} + \\ &\frac{\partial D(\mathbf{x}_{i,j,k})}{\partial x_2} \frac{\partial \mathbf{u}_{i,j,k}^t}{\partial x_2} + D(\mathbf{x}_{i,j,k}) \frac{\partial^2 \mathbf{u}_{i,j,k}^t}{\partial x_2^2} \\ &\frac{\partial D(\mathbf{x}_{i,j,k})}{\partial x_3} \frac{\partial \mathbf{u}_{i,j,k}^t}{\partial x_3} + D(\mathbf{x}_{i,j,k}) \frac{\partial^2 \mathbf{u}_{i,j,k}^t}{\partial x_3^2} + \rho \mathbf{u}_{i,j,k}^t (1 - \mathbf{u}_{i,j,k}^t), \end{aligned} \quad (4)$$

with

$$\begin{aligned} \frac{\partial \mathbf{u}_{i,j,k}^t}{\partial x_1} &= \frac{\mathbf{u}_{i+1,j,k}^t - \mathbf{u}_{i,j,k}^t}{h}, \\ \frac{\partial \mathbf{u}_{i,j,k}^t}{\partial x_2} &= \frac{\mathbf{u}_{i,j+1,k}^t - \mathbf{u}_{i,j,k}^t}{h}, \\ \frac{\partial \mathbf{u}_{i,j,k}^t}{\partial x_3} &= \frac{\mathbf{u}_{i,j,k+1}^t - \mathbf{u}_{i,j,k}^t}{h}, \\ \frac{\partial^2 \mathbf{u}_{i,j,k}^t}{\partial x_1^2} &= \frac{\mathbf{u}_{i+1,j,k}^t - 2\mathbf{u}_{i,j,k}^t + \mathbf{u}_{i-1,j,k}^t}{h^2}, \\ \frac{\partial^2 \mathbf{u}_{i,j,k}^t}{\partial x_2^2} &= \frac{\mathbf{u}_{i,j+1,k}^t - 2\mathbf{u}_{i,j,k}^t + \mathbf{u}_{i,j-1,k}^t}{h^2}, \\ \frac{\partial^2 \mathbf{u}_{i,j,k}^t}{\partial x_3^2} &= \frac{\mathbf{u}_{i,j,k+1}^t - 2\mathbf{u}_{i,j,k}^t + \mathbf{u}_{i,j,k-1}^t}{h^2}, \end{aligned} \quad (5)$$

and we obtain the following system of semilinear Ordinary Differential Equations

$$\begin{cases} \dot{\mathbf{U}}(t) = \mathbf{A}\mathbf{U}(t) + \mathbf{F}(\mathbf{U}(t)), & \text{in } I, \\ \mathbf{U}(0) = \mathbf{U}_0, \end{cases} \quad (6)$$

where $\mathbf{U}(t) = \{\mathbf{u}_{i,j,k}^t\}_{i=1,\dots,N_x; j=1,\dots,N_y; k=1,\dots,N_z}$ is the time-dependent vector of the degrees of freedom in space. To derive the \mathbf{A} operator, we simplify the

derivation, assuming $\frac{\partial D_{i,j,k}}{\partial x_i} = 0$,

$$\begin{aligned} \frac{\partial \mathbf{u}_{i,j,k}^t}{\partial t} &= D(x_{i,j,k}) \frac{\mathbf{u}_{i+1,j,k}^t - 2\mathbf{u}_{i,j,k}^t + \mathbf{u}_{i-1,j,k}^t}{h^2} \\ &+ D(x_{i,j,k}) \frac{\mathbf{u}_{i,j+1,k}^t - 2\mathbf{u}_{i,j,k}^t + \mathbf{u}_{i,j-1,k}^t}{h^2} \\ &+ D(x_{i,j,k}) \frac{\mathbf{u}_{i,j,k+1}^t - 2\mathbf{u}_{i,j,k}^t + \mathbf{u}_{i,j,k-1}^t}{h^2} + \rho \mathbf{u}_{i,j,k}^t (1 - \mathbf{u}_{i,j,k}^t), \end{aligned} \quad (7)$$

and we group the terms

$$\begin{aligned} h^2 \frac{\partial \mathbf{u}_{i,j,k}^t}{\partial t} &= -6D(x_{i,j,k}) \mathbf{u}_{i,j,k}^t + D(x_{i,j,k}) \mathbf{u}_{i-1,j,k}^t \\ &+ D(x_{i,j,k}) \mathbf{u}_{i,j-1,k}^t + D(x_{i,j,k}) \mathbf{u}_{i,j,k-1}^t \\ &+ D(x_{i,j,k}) \mathbf{u}_{i+1,j,k}^t + D(x_{i,j,k}) \mathbf{u}_{i,j+1,k}^t \\ &+ D(x_{i,j,k}) \mathbf{u}_{i,j,k+1}^t + h^2 \rho \mathbf{u}_{i,j,k}^t (1 - \mathbf{u}_{i,j,k}^t), \end{aligned} \quad (8)$$

The entries of matrix A are

$$A_{i,j,k;l,m,n} = \begin{cases} -6D(x_{i,j,k}), & (i,j,k) == (l,m,n), \\ D(x_{i-1,j,k}), & (l,m,n) \in \{(i-1,j,k), (i+1,j,k), \\ & (i,j-1,k), (i-1,j+1,k), \\ & (i-1,j,k-1), (i-1,j,k+1)\}, \\ 0, & \text{otherwise.} \end{cases} \quad (9)$$

We employ $\{1, \dots, N_x\} \times \{1, \dots, N_y\} \times \{1, \dots, N_z\} \ni (i, j, k) \rightarrow \text{global}(i, j, k) = i + (j-1)N_y + (j-1)(k-1)N_y N_z$ is the mapping from the integer coordinates into the global rows / columns numbering. The F operator is given by $F(\mathbf{U}(t)) = \rho \mathbf{U}(t)(1 - \mathbf{U}(t))$.

4. Exponential integrators

For the time discretization, we consider a uniform partition of the time interval as

$$0 = t_0 < t_1 < \dots < t_{N-1} < t_N = T, \quad (10)$$

we define $I_n = (t_n, t_{n+1})$ and $\tau = t_{n+1} - t_n$, $\forall n = 0, \dots, N-1$. Let \mathbf{U}_n be the numerical approximation to the solution of (6) at t_n , we know that

the integral representation of the solution of (6) at \mathbf{t}_{n+1} , also known as the *variation-of-constants* formula, reads

$$\mathbf{U}_{n+1} = e^{\tau\mathbf{A}}\mathbf{U}_n + \mathbf{h} \int_0^1 e^{(1-\theta)\tau\mathbf{A}} F(\mathbf{U}(\mathbf{t}_n + \tau\theta)) d\theta. \quad (11)$$

Different approximations of the nonlinear term in (11) lead to different exponential time integration methods [9]. All these methods are expressed in terms of the so-called φ -functions defined as

$$\begin{cases} \varphi_0(z) = e^z, \\ \varphi_p(z) = \int_0^1 e^{(1-\theta)z} \frac{\theta^{p-1}}{(p-1)!} d\theta, \quad \forall p \geq 1, \end{cases} \quad (12)$$

which satisfy the following recurrence relation

$$\varphi_{p+1}(z) = \frac{1}{z} \left(\varphi_p(z) - \frac{1}{p!} \right). \quad (13)$$

Here, we will focus on the simplest exponential integrator method, the *Exponential Euler* method, which is first order in time. For higher-order methods we refer to [9, 16]. For that, we approximate in (11) the non-linear term with its value at \mathbf{t}_n that it is known, i.e., $F(\mathbf{U}(\mathbf{t}_n + \tau\theta)) \approx F(\mathbf{U}_n)$. Integrating exactly in (11), we obtain

$$\mathbf{U}_{n+1} = \varphi_0(\tau\mathbf{A})\mathbf{U}_n + \tau\varphi_1(\tau\mathbf{A})F(\mathbf{U}_n). \quad (14)$$

which is given in terms of the φ -functions (12). Finally, employing the recurrence formula (13), we rewrite (14) as

$$\mathbf{U}_{n+1} = \mathbf{U}_n + \tau\varphi_1(\tau\mathbf{A})(F(\mathbf{U}_n) + \tau\mathbf{A}\mathbf{U}_n). \quad (15)$$

For the numerical results, we employ the *MATLAB* routines from [2] for computing the action of φ -functions over vectors. In this routine the authors employ the scaling and squaring method together with a truncated Taylor series approximation to the exponential of a matrix. As we show in the numerical results, this routine applied to operator $\tau\mathbf{A}$ coming from finite difference semidiscretization in space is extremely efficient. Moreover, exponential integrators are suitable for long-time simulations as they are unconditionally stable.

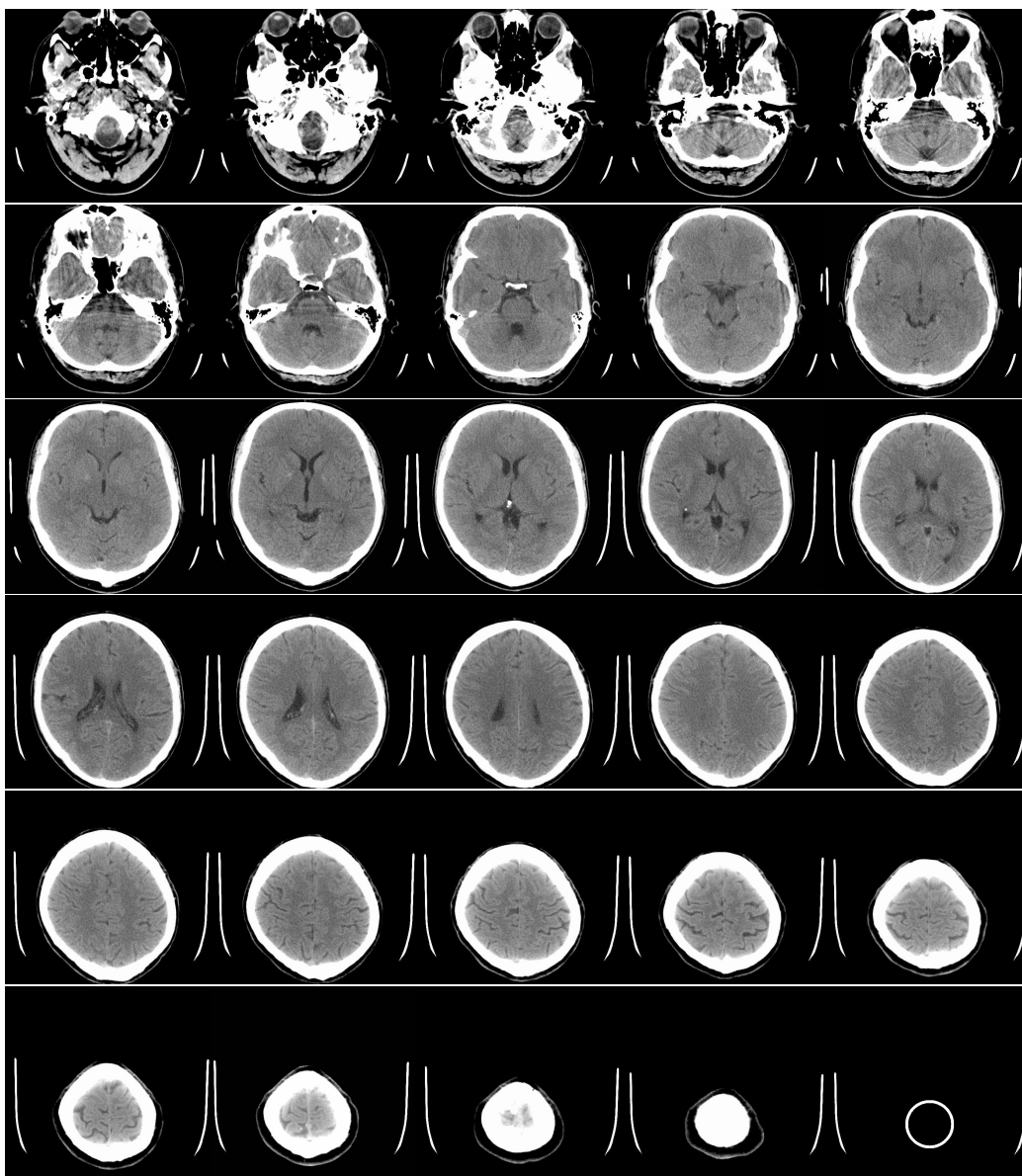


Figure 1: MRI scans of the head of Maciej Paszyński.

5. Numerical results

5.1. MRI scan of the human brain

Our simulations are based on digital data, the MRI scan with 29 two-dimensional slices, each one with 532 times 565 pixels. Each pixel's intensity is a value from the range of $[0, 255]$, and it's proportional to the material's (skull, skin, white matter or gray matter, and air) normalized density. Exemplary slices of the human head from the MRI scan of the head of one of the authors (Maciej Paszyński) are presented in Figure 1. Next, according to the MRI scan data, we employ material data changing on the skull, skin, white matter, gray matter, and air. We assume air (MRI scan data ≤ 1), white matter ($1 \leq \text{approximation} \leq 230$), grey matter ($230 < \text{approximation} \leq 240$) and skull (approximation > 240).

5.2. Two-dimensional glioblastoma brain tumor simulation

We consider one central slice of the MRI scan data. Let $\Omega \subset [0, 200]^2$ [mm^2] be an open set and $I = (150, 3500)$ [days] the simulated time interval. We solve the two-dimensional version of the Fisher-Kolmogorov diffusion-reaction equation with logistic growth describing the brain tumor dynamics (1) [21]. We prescribe the following initial state

$$\mathbf{u}(\mathbf{x}_1, \mathbf{x}_2; \mathbf{t}_0) = 0.1 \exp(-10((\mathbf{x}_1 - 110)^2 + (\mathbf{x}_2 - 140)^2)). \quad (16)$$

We select $\rho = 2.5 \times 0.01$ [days^{-1}] [6]. The diffusion coefficient for the white matter is defined as $D_w = 1.3 \times 0.1$ [$\text{mm}^2 \text{days}^{-1}$] [6]. The diffusion coefficient for the gray matter is defined as $D_w = 0.13 \times 0.1$ [$\text{mm}^2 \text{days}^{-1}$] [?].

With this parameters setup, we start from $\mathbf{t}_0 = 150$ [days] with $T = 3500$, and we perform 100 time steps of the exponential integrator simulation. Thus, one time step represents $\frac{3500-150}{100} = 33.5$ [days]. The spatial mesh consists of 193×193 points. The 100 time steps exponential integrators method executed on a laptop with Win10, using Octave, with 11th Gen Intel(R) Core(TM) i5-11500H @ 2.90GHz, 2.92 GHz, and 32 GB of RAM, takes less than 6 seconds. The selected snapshots from the simulation are presented in Figures 2-3. In these pictures, we do not present the brain tissue, just the density of the tumor cells.

This single two-dimensional slice of the human head has around 70 percent of the gray matter, and 30 percent of the white matter. According to our evaluation, we have the theoretical predicted tumor velocity as of $2\sqrt{D}\rho =$

0.11 [mm days⁻¹]. This means that we have 11mm progression per 100 days. The progression from day 150 (our initial state, where the tumor had a diameter of 1mm) to day 518, presented in Figures 2-3 shows the progression from 1mm to 42mm (as measuring the tumor radius in one dimension). This implies the tumor velocity of $\frac{42}{518-150} = 0.11$ [mm days⁻¹]. This confirms the agreement between the numerical results and the model setup.

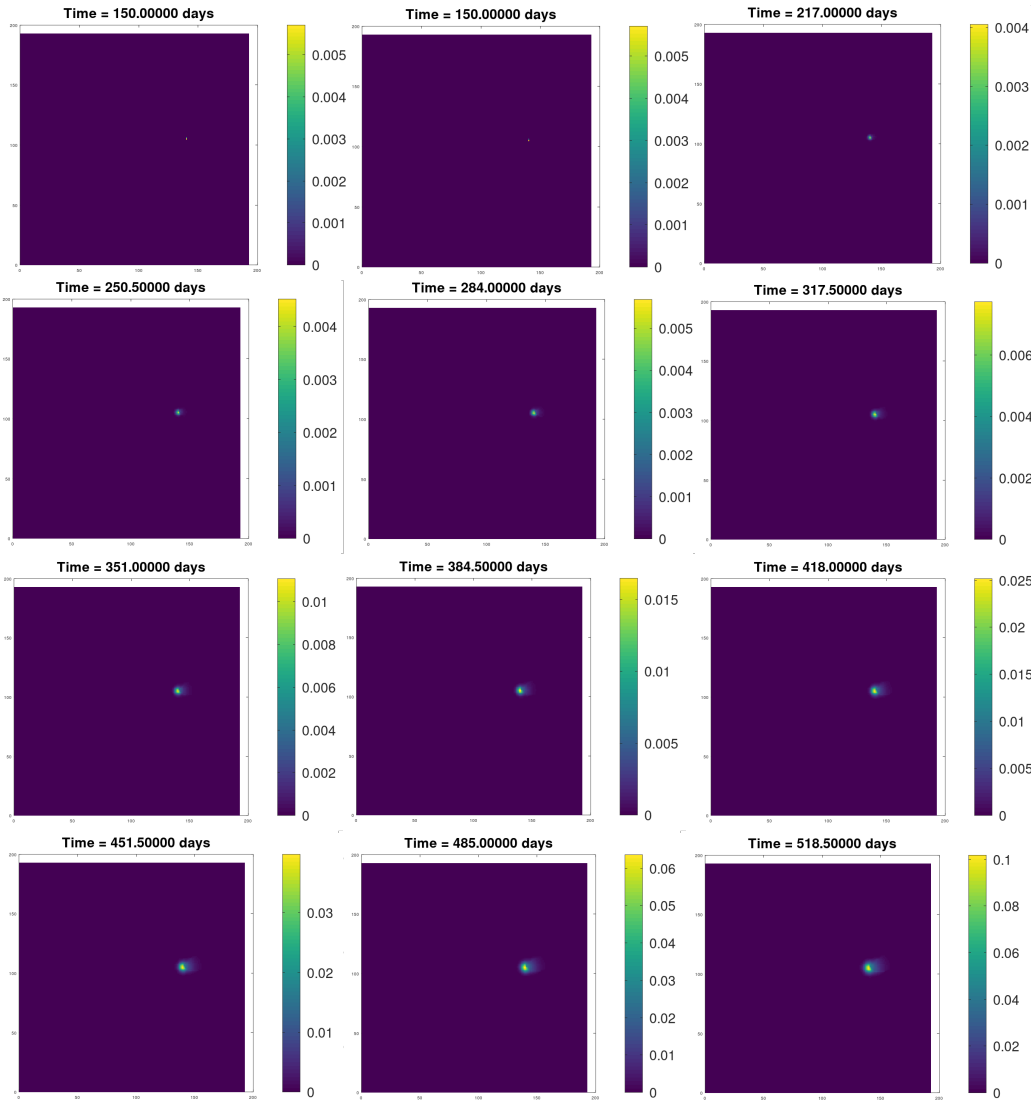


Figure 2: Sequence of snapshots from the two-dimensional tumor brain simulations.

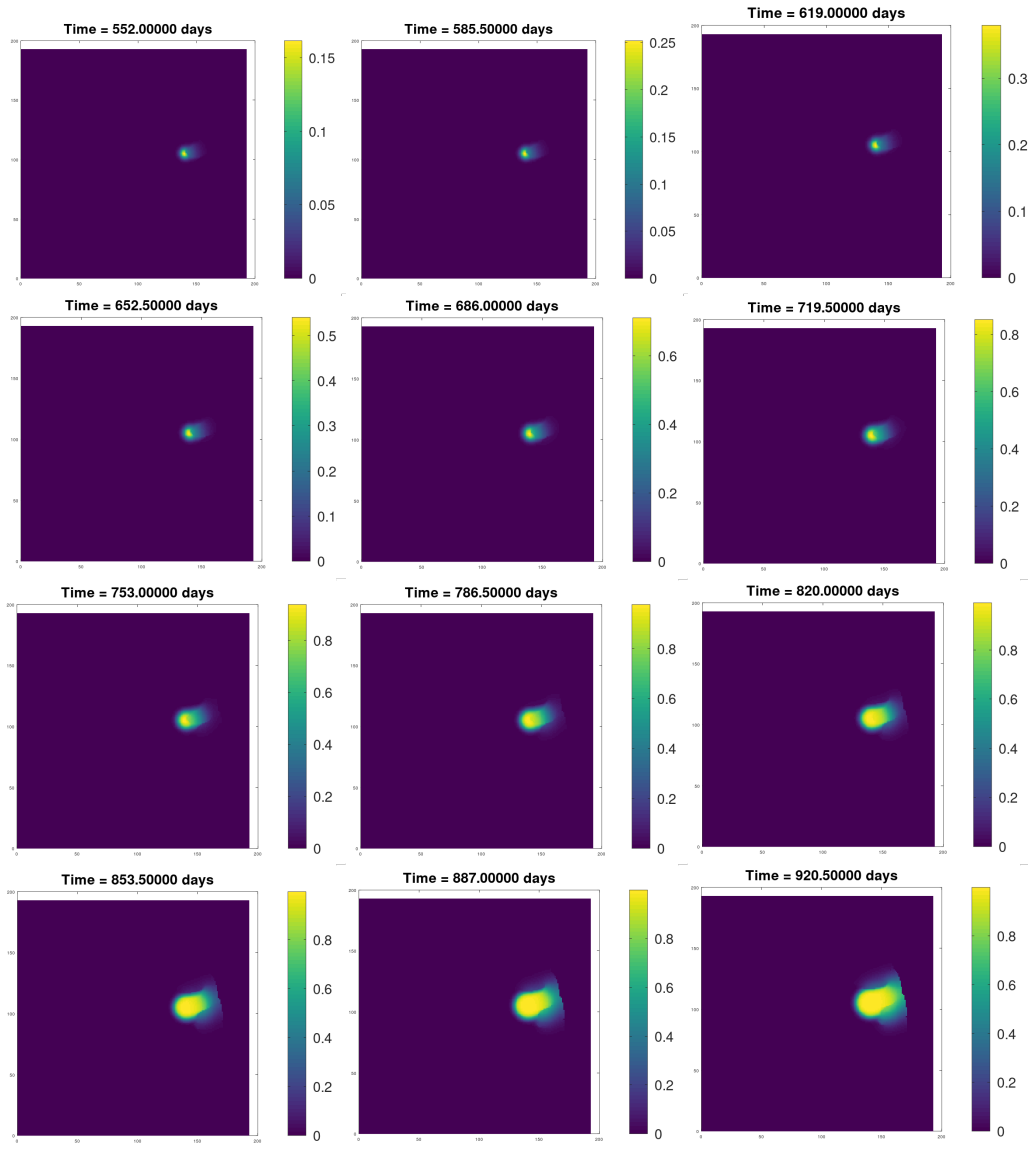


Figure 3: Sequence of snapshots from the two-dimensional tumor brain simulations. Continuation.

5.3. Three dimensional glioblastoma brain tumor simulation

We construct 3D computational grid out of 28 slices of the MRI scan. We want to solve the Fisher-Kolmogorov diffusion-reaction equation with logistic growth (1) describing the brain tumor dynamics [21] over $\Omega \subset [0, 200]^3$

[mm³], and time interval $I = (150, 3500)$ [days] and prescribed initial state

$$\mathbf{u}(x_1, x_2, x_3; t_0) = 0.1 \exp(-10((x_1 - 102)^2 + (x_2 - 138)^2 + (x_3 - 96)^2)) \quad (17)$$

Following [6?] we consider $\rho = 2.5 \times 0.01$ [days⁻¹]. $D_w = 1.3 \times 0.1$ [mm²days⁻¹] [6]. $D_g = 0.13 \times 0.1$ [mm²days⁻¹]. We perform 100 time steps, starting from $t_0 = 150$ [days], with time step = 33.5 [days]. The spatial mesh consists of $50 \times 50 \times 50$ points. The 100 time steps exponential integrators method executed on a laptop with Win10, using Octave, with 11th Gen Intel(R) Core(TM) i5-11500H @ 2.90GHz, 2.92 GHz and 32 GB of RAM, takes less than 3 seconds. The selected snapshots from the simulation are presented in Figure 4-6. We show the brain tissue and the growing tumor cells. The visualization has been performed through the interface with ParaView [1].

The percentage of the gray matter and white matter in the full three-dimensional MRI scan of the human head is around 85 percent of the gray matter, and 15 percent of the white matter. This implies the following theoretical predicted tumor velocity as of $2\sqrt{D}\rho = 2\sqrt{p_w D_w + p_g D_g}\rho = 0.087$ [mm days⁻¹]. This means that we have 9mm progression per 100 days.

The progression from day 150 (our initial state, where the tumor had a diameter of 1mm) to day 485, presented in Figure 4 shows the progression from 1mm to 29mm (as measuring the tumor radius in one dimension) . This implies the tumor velocity of $\frac{28}{485-150} = 0.083$ [mm days⁻¹].

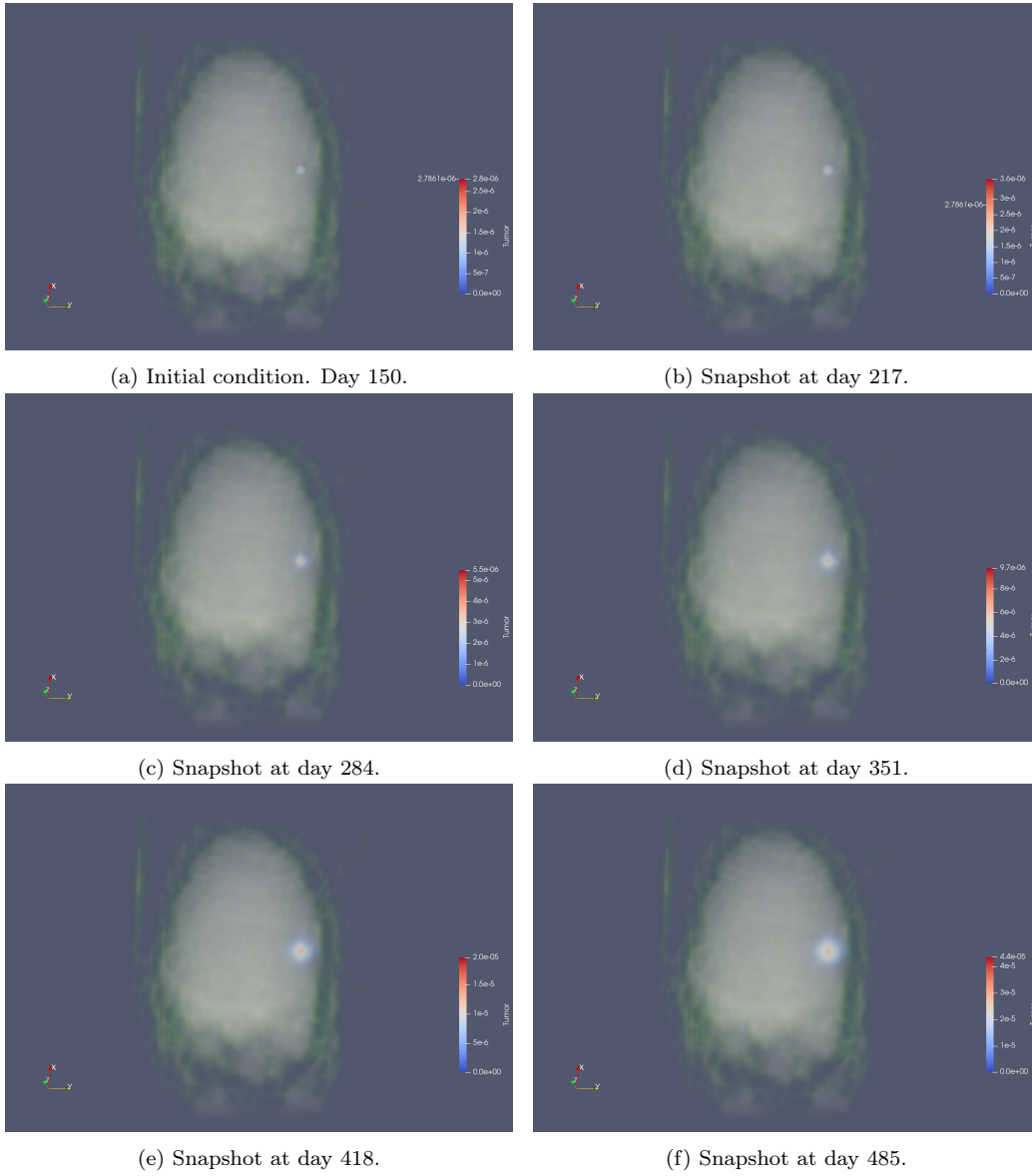


Figure 4: Sequence of snapshots from the 3D tumor brain simulation. Top view. Snapshots from day 150 (initial state), one time step is 33 days. Each snapshot is two time steps.

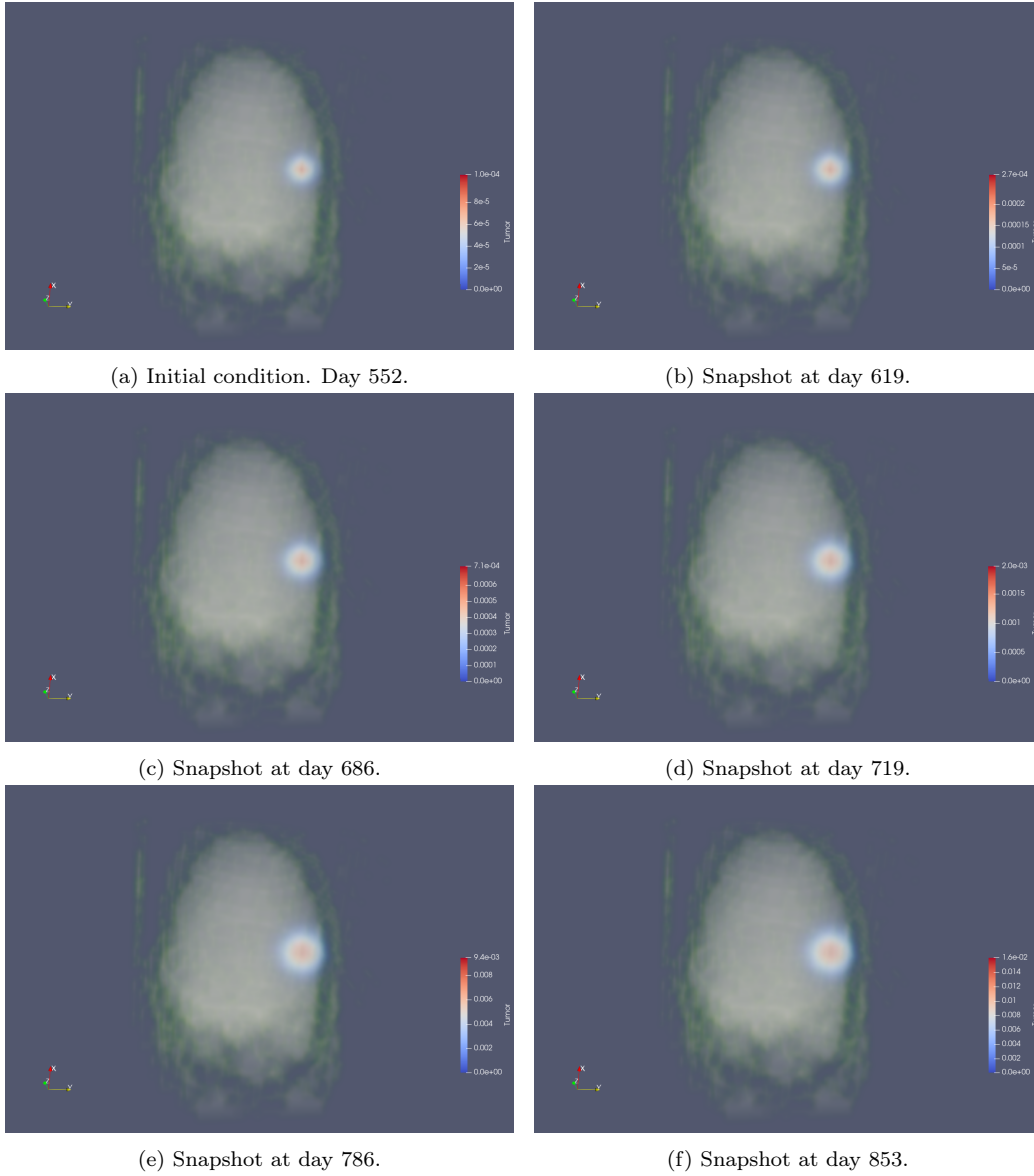


Figure 5: Sequence of snapshots from the 3D tumor brain simulation. Top view. Continuation from day Snapshots from day 552, one time step is 33 days. Each snapshot is two time steps.

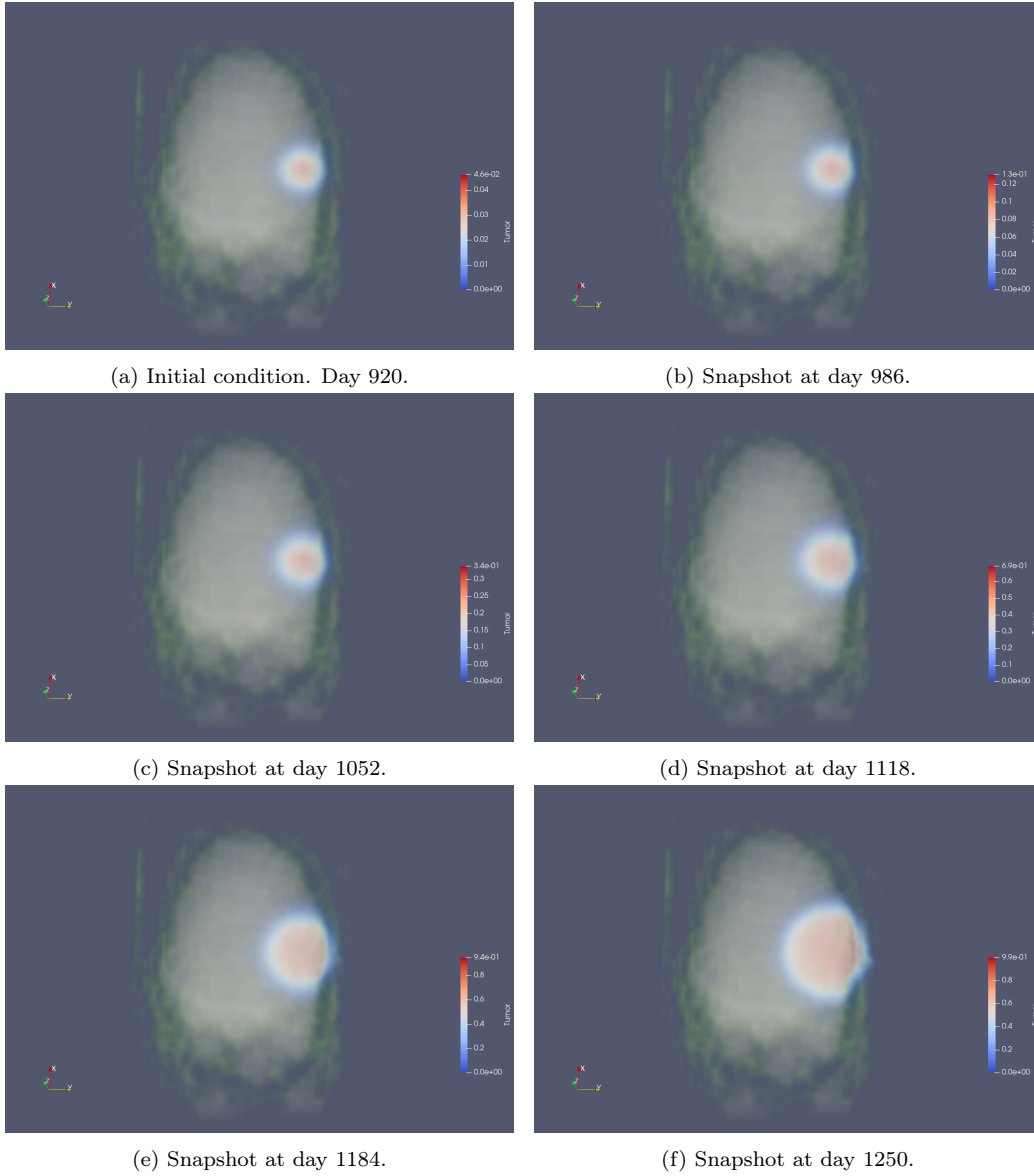


Figure 6: Sequence of snapshots from the 3D tumor brain simulation. Top view. Continuation from day Snapshots from day 920, one time step is 33 days. Each snapshot is two time steps.

6. Conclusions

Based on three-dimensional MRI scans of the human head, we build an ultra-fast simulator of brain tumor growth. We employed the Fisher-Kolmogorov diffusion-reaction equation with logistic growth to model the glioblastoma tumor. We used the exponential integrators method, employing the routine from [2] to compute the action of the exponentials, with a finite difference discretization in space. Our two-dimensional simulator written in Octave can predict a one-year forward tumor evolution within 6 seconds using the resolution of 193×193 pixels of a single two-dimensional slice of the human head. We also developed a three-dimensional simulator with Octave and ParaView visualization. The three-dimensional simulator on a laptop can perform a one-year tumor growth prediction with a resolution of $32 \times 32 \times 32$ pixels within 3 seconds. For both two-dimensional and three-dimensional simulations, we set the parameters of the simulator based on the average percentage of white and gray matter. With good agreement, we have compared the average velocity of the tumor growth resulting from the numerical experiments with the velocity predicted by the theory. As future work we plan analysis of the concurrency of the exponential integrators algorithm and development of a parallel version of the simulator, targeting GPGPU computing cards. Having the parallel simulator we will run large simulations on high-resolution human brain data. Another future direction of our research is the incorporation of the drug delivery term into our model [15]. In particular we plan to focus on the chemotherapy modeling. We also plan to address the data assimilation problem using the supermodeling technique [17, 19].

Acknowledgements

This work was partially supported by the program "Excellence initiative - research university" for the AGH University of Kraków. Judit Muñoz-Matute has received funding from the European Union's Horizon 2020 research and innovation programme under the Marie Skłodowska-Curie individual fellowship grant agreement No. 101017984 (GEODPG).

References

- [1] Ahrens, J., Geveci, B. & Law, C. ParaView: An End-User Tool for Large Data Visualization. *Visualization Handbook*. (2005), ISBN 978-0123875822
- [2] Al-Mohy, A. & Higham, N. Computing the action of the matrix exponential, with an application to exponential integrators. *SIAM Journal On Scientific Computing*. **33**, 488-511 (2011)
- [3] Cai, S., Mao, Z., Wang, Z., Yin, M. & Karniadakis, G. Physics-informed neural networks (PINNs) for fluid mechanics: A review. *Acta Mechanica Sinica*. **37**, 1727-1738 (2021)
- [4] Chen, Y., Lu, L., Karniadakis, G. & Dal Negro, L. Physics-informed neural networks for inverse problems in nano-optics and metamaterials. *Optics Express*. **28**, 11618-11633 (2020)
- [5] Croci, M. & Muñoz-Matute, J. Exploiting Kronecker structure in exponential integrators: Fast approximation of the action of ϕ -functions of matrices via quadrature. *Journal Of Computational Science*. **67** pp. 101966 (2023), <https://www.sciencedirect.com/science/article/pii/S1877750323000261>
- [6] Harpold, H., Alvord, E. & Swanson, K. The evolution of mathematical modeling of glioma proliferation and invasion. *Journal Of Neuropathology And Experimental Neurology*. **66**, 1-9 (2007)
- [7] Hertler, C., Felsberg, J., Gramatzki, D., Le Rhun, E., Clarke, J., Soffietti, R., Wick, W., Chinot, O., Ducray, F., Roth, P., McDonald, K., Hau, P., Hottinger, A., Jaap, R., Schnell, O., Marosi, C., Glantz, M., Darlix, A., Lombardi, G., Krex, D., Glas, M., Reardon, D., Bent, M., Lefranc, F., Herrlinger, U., Razis, E., Carpentier, A., Phillips, S., Rudà, R., Wick, A., Tabouret, E., Meyronet, D., Maura, C., Rushing, E., Rapkins, R., Bumès, E., Hegi, M., Weyerbrock, A., Aregawi, D., Gonzalez-Gomez, C., Pellerino, A., Klein, M., Preusser, M., Bendszus, M., Golfopoulos, V., Deimling, A., Gorlia, T., Y. Wen, P., Reifenberger, G. & Weller, M. Long-term survival with IDH wildtype glioblastoma: first results from the ETERNITY Brain Tumor Funders' Collaborative Consortium (EORTC 1419). *European Journal Of Cancer Research*. **189** (2023)

- [8] Hochbruck, M. & Ostermann, A. Explicit exponential Runge–Kutta methods for semilinear parabolic problems. *SIAM Journal On Numerical Analysis*. **43**, 1069-1090 (2005)
- [9] Hochbruck, M. & Ostermann, A. Exponential integrators. *Acta Numerica*. **19** pp. 209-286 (2010)
- [10] Hogue, C., Davatzikos, C. & Biros, G. An image-driven parameter estimation problem for a reaction–diffusion glioma growth model with mass effects. *Journal Of Mathematical Biology*. **56** pp. 793-825 (2008)
- [11] Kłusek, A., Łoś, M., Paszyński, M. & Dzwinel, W. Efficient model of tumor dynamics simulated in multi-GPU environment. *The International Journal Of High Performance Computing Applications*. **33**, 489-506 (2019)
- [12] Lipková, J., Angelikopoulos, P., Wu, S., Alberts, E., Wiestler, B., Diehl, C., Preibisch, C., Pyka, T., Combs, S., Hadjidakas, P., Leemput, K., Koumoutsakos, P., Lowengrub, J. & Menze, B. Personalized Radiotherapy Design for Glioblastoma: Integrating Mathematical Tumor Models, Multimodal Scans, and Bayesian Inference. *IEEE Transactions On Medical Imaging*. **38** pp. 1875-1884 (2018)
- [13] Maddalena, L. & Ragni, S. Existence of solutions and numerical approximation of a non-local tumor growth model. *Mathematical Medicine And Biology: A Journal Of The IMA*. **37**, 58-82 (2020)
- [14] Menze, B. H., Van Leemput, K., Honkela, A., Konukoglu, E., Weber, M.-A. , Ayache, N. & Golland, P. A generative approach for image-based modeling of tumor growth. In G. Székely and H. K. Hahn, editors, *Information Processing in Medical Imaging*, 735–747, Berlin, Heidelberg (2011)
- [15] McDaniel, J., Kostelich, E., Kuang, Y., Nagy, J., Preul, M., Moore, N. & Matirosyan, N. Data Assimilation in Brain Tumor Models. *Mathematical Methods And Models In Biomedicine*. pp. 233-262 (2013)
- [16] Muñoz-Matute, J. & Demkowicz, L. Multistage DPG time-marching scheme for nonlinear problems. *ArXiv Preprint arXiv:2309.00069*. (2023)

- [17] Paszyński, M., Siwik, L., Dzwinel, W. & Pingali, K. Supermodeling, a convergent data assimilation meta-procedure used in simulation of tumor progression. *Computers & Mathematics With Applications*. **113** pp. 214-224 (2022)
- [18] Raissi, M., Perdikaris, P. & Karniadakis, G. Physics-informed neural networks: A deep learning framework for solving forward and inverse problems involving nonlinear partial differential equations. *Journal Of Computational Physics*. **378** pp. 686-707 (2019)
- [19] Siwik, L., Łoś, M., Kłusek, A., Paszyńska, A., Pingali, K., Dzwinel, W. & Paszyński, M. Tuning three-dimensional tumor progression simulations on a cluster of GPGPUs. *Journal Of Computational And Applied Mathematics*. **412** pp. 114308 (2022)
- [20] Stupp, R., Brada, M., Van den Bent, M., Tonn, J., Pentheroudakis, G. & ESMO Guidelines Working Group High-grade glioma: ESMO clinical practice guidelines for diagnosis, treatment and follow-up. *Annals Of Oncology*. **25** pp. 93-101 (2014,9)
- [21] Swanson, K., Alvord Jr, E. & Murray, J. A quantitative model for differential motility of gliomas in grey and white matter. *Cell Proliferation*. **33**, 317-329 (2000)
- [22] Zhu, A. Accelerating Parameter Inference in Diffusion-Reaction Models of Glioblastoma Using Physics-Informed Neural Networks. (SIAM Undergraduate Resources Online,2022)
- [23] Łoś, M., Kłusek, A., Hassaan, M., Pingali, K., Dzwinel, W. & Paszyński, M. Parallel fast isogeometric L2 projection solver with GALOIS system for 3D tumor growth simulations. *Computer Methods In Applied Mechanics And Engineering*. **343** pp. 1-22 (2019)
- [24] Łoś, M., Paszyński, M., Kłusek, A. & Dzwinel, W. Application of fast isogeometric L2 projection solver for tumor growth simulations. *Computer Methods In Applied Mechanics And Engineering*. **316** pp. 1257-1269 (2017), Special Issue on Isogeometric Analysis: Progress and Challenges